COMPARATIVE FIRST-PRINCIPLES MOLECULAR DYNAMICS STUDY OF TIN(001)/SIN/TIN(001) AND TIN(001)/SIC/TIN(001) INTERFACES IN SUPERHARD NANOCOMPOSITES

Volodymyr Ivashchenko[1*], Stan Veprek[2], Volodymyr Shevchenko[1]

1 Institute of Problems of Material Science, NAS of Ukraine, Krzhyzhanovsky str. 3, 03142 Kyiv, Ukraine
2 Department of Chemistry, Technical University Munich, Lichtenbergstrasse 4, D-85747 Garching, Germany

ABSTRACT

Heterostructures TiN(001)/SiN/TiN(001) and TiN(001)/SiC/TiN(001), with one monolayer (ML) of interfacial SiN and SiC, respectively, inserted between five monolayer thick B1-TiN, were investigated using first-principles quantum molecular dynamics (QMD) calculations. The temperature dependent QMD simulations at 300 K in combination with subsequent variable-cell structural relaxation revealed that the TiN(001)/SiN/TiN(001) interface exists as pseudomorphic B1-SiN layer only at 0 K, and as a superposition of distorted octahedral SiN_6 and tetrahedral SiN_4 units aligned along the (110) direction at a finite temperature. Thus, at 300 K, the interfacial layer is not epitaxial. Instead it consists of aggregates of the B1-SiN-like and Si_3N_4-like distorted clusters. However, in the the TiN(001)/SiC/TiN(001) heterostructures, the interfacial layer remains epitaxial B1-SiC at 0 K as well as at 300 K, with only a small shift of nitrogen atoms on both sides of the interface towards the silicon atoms. A comparison with the results obtained by earlier "static" *ab initio* DFT calculations at 0 K shows the great advantage of the QMD calculations that allow us to reveal structural reconstructions caused by thermal activation.

Key words: nanocomposite, interface, first-principles investigation, quantum molecular dynamics

INTRODUCTION

Large experience in the design of superhard nanocomposites and heterostructures, and understanding of their properties has been achieved during the last decade. Among them, TiN/SiN nanocomposites represent the most studied system. They exhibit superhardness (40-100 GPa) combined with high thermal stability and oxidation resistance [1-5]. The strong increase of hardness as compared with pure TiN coatings (20-21 GPa) has been explained by the nanometer size, the randomly oriented TiN grains which prevent dislocation nucleation and motion and 1 monolayer thick (1 ML) SiN_x interfacial layer that is

* e-mail: ivash@ipms.kiev.ua, tel: (+38)0443901135 tel: (+38)0501442687

strengthened by valence charge transfer which reduces grain boundary shear [6]. When the thickness of the SiN_x layer increases above about 1 ML the hardness enhancement decreases because of the weakening of the adjacent Ti-N bonds [7]. The 1 ML thick SiN_x interfacial layer appears X-ray amorphous because of the random orientation of the TiN nanocrystals.

The possibility of the formation of an epitaxial interfaces in TiN/SiN_x heterostructures was considered in Ref. [8-13]. Hultman, Bareno, Flink et al. showed experimentally that the SiN_x tissue can be crystalline provided its thickness does not exceed a few monolayers [9]. The investigations of the TiN(001)/SiN nanolaminates with the thicknesses of SiN_x layers, $l_{SiN} < 9$ Å showed that the SiN_x layers were epitaxial cubic, but it became amorphous when l_{SiN} exceeded > 9 Å [8]. Hu et al. [12] showed that SiN_x, being amorphous in a thick monoblock film, formed a crystalline structure in TiN/ SiN_x multilayers when the thickness of the SiN_x layers was less than 7 Å because of the "template effect". Iwamoto and Tanaka investigated the TiN/Si_3N_4 interface and found that the TiN nanocrystals extended along (0001) axis of Si_3N_4 with the (110) direction of TiN being parallel to the (0001) direction of Si_3N_4 [13].

Both the coherent and incoherent TiN/SiN_x interfaces were widely investigated in the framework of different first-principles procedures [6,7,14-20]. It was shown that the epitaxial structure of the TiN(111)/B1-SiN and TiN(110)/B1-SiN interfaces was preserved after the structural relaxation under the periodic boundary conditions, whereas the TiN(001)/B1-SiN became stable only after a distortion of the Si-atoms in the [110] direction by about 12 % [6,7,14]. The topology of the semicoherent TiN(111)/β-Si_3N_4 interface was found to change by forming a plane containing Si-Si bonds which were lacking in the initial structure before relaxation [6]. Zhang et al. [15] showed that the (111) and (110) B1-SiN-like interfaces are stable, while the (001) fcc-SiN interface is unstable against finite distortions. Later on, it was established that the distorted (001) and the undistorted (111) interface are also dynamically stable [16,17]. However, both interfaces are unstable with respect to formation of Si vacancies [17]. The stability of different TiN(111)/SiN_x heterostructures including the TiN(111)/Si_3N_4(10-10) interface was theoretically investigated in Refs. [18-20]. DFT calculations of various SiN_x interface configurations between two ten-layer TiN(111) slabs showed that, for nitrogen-rich conditions, a so-called β-like (1×3)-Si_2N_3 structure involving tetrahedral N-Si-N bonding was most favorable, while for nitrogen-poor conditions a (1×1)-TiSi structure with octahedral Ti-Si-Ti bonding was preferred [19]. It was found also [19] that the Si-N bonds in the 1 ML thick β-like Si_2N_3 interface are stronger than in the (10-10) oriented bulk β-Si_3N_4.

It should be emphasized that all the above mentioned theoretical structural investigations on the TiN/SiN interfaces were done by means of geometry optimization at 0 K, and the TiN/SiC interfaces were not investigated at all. In the

present paper, we conduct a comparative study of the TiN(001)/SiN and TiN(001)/SiC interfaces using first-principles quantum molecular dynamics (QMD) simulations.

COMPUTATATIONAL ASPECTS

The present calculations were done using the first-principles pseudo-potential DFT MD method as implemented in the quantum ESPRESSO code [21] with periodic boundary conditions. The generalized gradient approximation (GGA) of Perdew, Burke and Ernzerhof [22] has been used for the exchange-correlation energy and potential, and the Vanderbilt ultra-soft pseudo-potentials were used to describe the electron-ion interaction [23]. In this approach, the orbitals are allowed to be as soft as possible in the core regions so that their plane-wave expansion converges rapidly [23]. The non-linear core corrections were taken into account as described in [21]. The criterion of convergence for the total energy was 10^{-6} Ry/formula unit. To speed up the convergence, each eigenvalue was convoluted with a Gaussian of a width of σ = 0.02 Ry. In molecular dynamics simulations only the Γ point was taken into account in the Brillouin zone (BZ) integration, and the cut-off energy for the plane-wave basis was set to 24 Ry.

For calculations of the SiN (SiC)-based heterostructures, we considered (2×2×3) 96-atom supercells constructed of the 8-atom B1-TiN cubic unit cells. The interfacial SiN and SiC monolayers have been introduced by replacing Ti atoms with Si and C atoms, respectively, in the central lattice plane of the given supercell. All the heterostructures consist of the six parallel layers aligned perpendicularly the c-direction, and one of them is the Si- or C-based interfacial layer.

All the initial structures were optimized by simultaneously relaxing the atomic basis vectors and the positions of atoms inside the unit cells using the Broyden-Fletcher-Goldfarb-Shanno (BFGS) algorithm [24]. The cut-off energy for the plane-wave basis $E_{cut\,=}$ 30 Ry and the Monkhorst-Pack [25] (2 2 2) mesh (four k-points) were used. The relaxation of the atomic coordinates and of the unit cell was considered to be complete when the atomic forces were less than 1.0 mRy/Bohr, the stresses were smaller than 0.05 GPa, and the total energy during the structural optimization iterative process was changing by less than 0.1 mRy/unit cell. The optimized interfacial TiN/SiN and TiN/SiC structures at zero temperature are denoted as ZT-SiN and ZT-SiC, respectively. Those calculated at 300 K ("low temperature") are denoted LT. The QMD optimization of the initial ZT heterostructures were carried out with fixed unit cell parameters and volume (the "NVT ensemble", constant number of particles, volume and temperature) for 2.5-2.7 ps. The system temperature was kept constant by rescaling the velocity. After the QMD equilibration at 300 K, the geometry of

all the heterostructures was optimized using the BFGS algorithm for variable cell dynamics [24] under conditions described above.

In large-supercell calculations, the chosen reduced energy cut-off and the mesh of k-points were used in order to spare computing time without compromising accuracy. We have chosen them after having verified the accuracy of the lattice parameter a and bulk modulus B for TiN: For the 96-atom sample with E_{cut} = 24 Ry and the one k- point, we obtained a = 4.228 Å and B = 276 GPa, whereas with E_{cut} = 30 Ry and the (2 2 2) mesh, the lattice constant and bulk modulus were 4.248 Å and 278 GPa, respectively, which is a very good agreement. For the 2-atom TiN cell with E_{cut} = 30 Ry and the (8 8 8) mesh, our calculated lattice constant was a = 4.249 Å and bulk modulus B = 273 GPa. The calculated lattice constants are close to the experimental value of 4.24 Å and comparable with other theoretical results of 4.239-4.275 Å [26]. The bulk moduli are consistent with the experimental and theoretical values of 264-326 GPa [26]. We compared also the total energy of pure TiN obtained for the 96-atom unit cell with E_{cut} =30 Ry and (2 2 2) mesh with 2-atom cell, E_{cut} = 30 Ry and the (8 8 8) mesh. The total energy difference was only about 0.3 mRy/formula unit.

The structural optimizations were carried out for the equilibrated structures. We have controlled the variation of total energy during each QMD time step. During the initial 1 to 1.5 ps, all structures reached closely their equilibrium state and, afterwards, the total energy of the equilibrated structures varied only slightly around the constant equilibrium value with a small amplitude of 0.37 mRy/atom. We have verified the convergence of the final relaxed structure in dependence on the simulation time and the total energy of an equilibrated structure by choosing two SiN-based heterostructures at the later stages of simulation with simulation time and total energy differences of 0.2 ps and 0.74 mRy/atom, respectively. Their pair correlation functions and atomic configurations practically coincided, and the total energy difference was only about 0.27 mRy/unit cell. This shows that the resultant relaxed structures are only very weakly sensitive to structural changes during the last stage of the QMD simulation.

We have also carried out QMD calculations using a smaller cell of 64 atoms and obtained essentially the same results to be reported below for the large cell of 96 atoms. Thus, the 96-atom unit cells are quite appropriate for QMD simulations of the TiN/1 ML SiN/TiN and TiN/1ML SiC/TiN heterostructures.

RESULTS AND DISCUSSION

Before the discussion of the computed results, a brief remark should be made: In order to simulate the interface structures it were appropriate to model the sequential deposition of the TiN and SiN layers. However, a very large scale MD simulation had to be used in such case, which it is impossible in the

framework of a first-principles procedure. Such large-scale simulations could be carried out using reliable empirical potentials, which are however lacking for the Ti-Si-C-N system. Therefore, we considered the evolution of the given structure of the epitaxial B1-SiN and B1-SiC layers between the B1-TiN layers at a finite temperature, which enabled us to analyze the atomic configurations of the interfaces and their stability as function of temperature.

First we performed geometry optimization of the initial epitaxial heterostructures at zero temperature. The epitaxial arrangement was found to be preserved for all interfaces. *Figure 1* shows the atomic configurations of the TiN(001)/SiN/TiN(001) and TiN(001)/SiC/TiN(001) heterostructures after initial optimization (ZT) and after QMD simulations at 300 K with subsequent variable-cell structural relaxation (LT). *Figure 2* shows the arrangement of the atoms located on the interfacial planes. A visual inspection of the atomic configurations allows the following conclusions. For the SiN-based interfaces, we note significant changes in the atomic arrangement induced by thermal motion of the interfacial atoms. The atomic redistribution occurs mostly at the interfaces. We also note the symmetrical shift of the N atoms toward the interfacial layer due to the higher electronegativity of Si as compared with Ti. The shifts of the Si atoms within the interface lead to a loss of part of the bonds of the original fcc-like structure. Most remarkable is the formation of the SiN_4 and NSi_6 units aligned along the (110) direction (cf. Fig. 2).

The thermal energy supplied to the TiN(001)/SiN heterostructure at 300 K is sufficient for the formation of the new Si_3N_4-like fragments at the interface. Thus, the TiN(001)/SiN/TiN(001) interface exists as pseudomorphic B1-SiN layer only at 0 K, but as a superposition of distorted octahedral SiN_6 and tetrahedral SiN_4 units aligned along the (110) direction at the finite temperature.

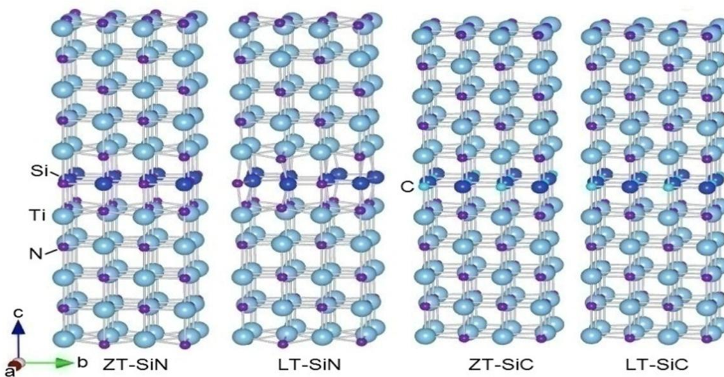

Fig. 1. (Color online) Atomic configuration of the zero- and low-temperature TiN/1 ML SiN (SiC)/TiN heterostructures (see text), which were calculated using the Si-N, Si-C and Ti-N bond length cutoffs of 2.5 Å

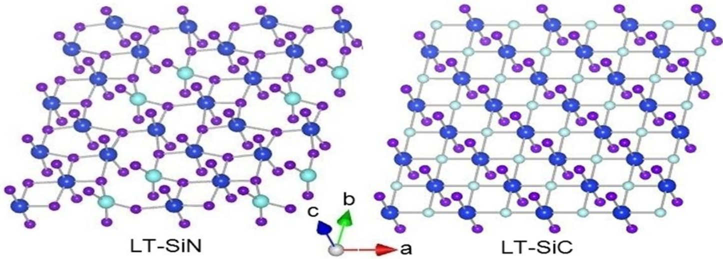

Fig. 2. (Color online) Atomic configurations in and around the interfacial planes, which were calculated using the Si-N and SiC bond length cutoff of 2.5 Å. The light-colored small and large symbols are the carbon and four-fold coordinated Si atoms, respectively.

We see that the TiN(001)/SiC/TiN(001) interface preserves the epitaxial structure at both 0 K and 300 K. This interface represents the B1-SiC layer, and the Si atoms form the bonds with the nitrogen atoms at the neighboring layers that are slightly shorter compared to the Si-C bonds at the interface.

In *Fig. 3* we show the pair correlation function of the low-temperature heterostructures. One can see that the Ti-N network is preserved in both heterostructures, although, in the LT-SiN, it is more distorted than in the LT-SiC. The shift of Si atoms within the LT-SiN interface leads to shortening of the Ti-Si distances, which reflects the strengthening of the Ti-Si interaction. These interactions are seen in the PCF as the peak of the Ti-Si nearest neighbor correlations at 2.75-2.82 Å. These values compare with the experimental Ti-Si bond lengths of 2.54-2.76 Å found for $TiSi_2$ (space group Fddd, No. 70, X-ray powder diffraction file [065-2522]). In the case of the LT-SiC interface, such interactions were not found (cf. *Fig. 3*).

Very interesting is the PCF for the Si-Si bonds and distances. As one can see in *Fig. 3*, there is one peak at distance of about 3 Å in the LT-SiC that corresponds to the nearest neighbor (Si-Si) correlations in the interfaces. Because this interface is stable, there is no noticeable difference between the ZT and LT case (cf. *Fig. 1*). In contrast, this peak splits into several shoulders in the case of the LT-SiN interface due to the random distortion as discussed above. This splitting is characterized by an appearance of a new peak at about 2.7 Å, which corresponds to the weak Si-Si bonds. This can be understood on the basis of thermodynamic instability of SiN which, in the case of closed system as simulated by the QMD, should decompose according to 4SiN $\rightarrow$ Si_3N_4 + Si with a high Gibbs free energy of the reaction of -136.3 kJ/mol of atoms [27]. Obviously, there is a kinetic activation barrier for this reaction to occur at room temperature. Therefore this PCF peak is located at longer distances compared with the Si-Si bond length in crystalline and amorphous silicon (2.35Å). Because the Si-N bond length of 1.75Å in β-Si_3N_4 is much shorter than the Ti-N bond length of 2.12 Å in pure TiN, there is a tensile misfit stress within the interfaces.

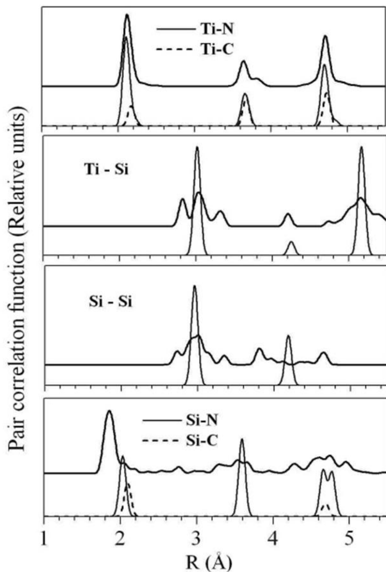

Fig. 3. Partial pair correlation function of the LT-SiN (upper curves) and LT-SiC (low curves) heterostructures

This stress and the tendency of silicon to attain its four-fold coordination to nitrogen as in Si_3N_4, which is the most stable configuration in the Si-N system, are the main factors that cause the reconstruction of the epitaxial layers. Figure 3 shows that the Si-N bonds are shorter than the Ti-N bonds in all heterostructures, and this tendency to shortening is more pronounced for the LT-SiN interface. For this interface, the one-peak Si-N nearest neighbor correlation with the elongated Si-N bonds around 1.85 Å is seen. An inspection of the atomic arrangement and the PCF for the LT-SiN clearly shows that the bond lengths of 1.76-1.85 Å correspond to the Si-N bonds in the distorted β-Si_3N_4–like units, whereas the peak located at higher distances corresponds to the Si-N bond lengths in the SiN_6 units. The shortening of the Si-N bonds causes an elongation of the Ti-N ones: the average length of the Ti-N bonds adjacent to the interfacial LT-SiN layer is 2.206 Å. The average length of the Ti-N bonds between the next neighbor planes parallel to the LT-SiN interface is about 2.07 Å. Thus, the broadening of the PCF peaks of the Ti-N next-near neighbor peaks seen in Fig. 3 is due to this bond length distribution. For the LT-SiC, the lengths of bonds change in the Si-N-Ti-N chain along the c-axis as 2.03, 2.217, 2.150 Å, and in the C-Ti-N-Ti chain as 2.167, 2.120, 2.110 Å, respectively.

CONCLUSIONS

We performed first-principles quantum molecular dynamics calculations of the TiN(001)/B1-SiN/TiN(001) and TiN(001)/B1-SiC/TiN(001) heterostructures in order to clarify the interfacial layer stability at finite temperature. It was shown that the 1ML SiN heteroepitaxial layers were preserved during the structural optimization at 0 K in agreement with the earlier "static" DFT calculations of Zhang et al. However, when equilibrated at 300 K, the B1-SiN(001) interface reconstructed to an over-coordinated a-SiN-like structure. The interface consist of the distorted octahedral SiN_6 and tetrahedral SiN_4–like units aligned along the (110) direction. In contrast, the SiC(001) interface was stable at 0 K

as well as after heating to 300 K, showing only small distortions of the atoms from their fully symmetric position but preserving the local coordination. An increase of the Ti-N interplanar bond lengths near the interfaces has been found for the SiN interface associated with a shortening the Si-N bonds after interface reconstruction, in agreement with the Friedel-like oscillations reported by Zhang et al. in their DFT calculations at 0 K. Such Friedel-like oscillations are absent in the SiC-based heterostructures.

Acknowledgements

This work was supported by the STCU Contract, No. 4682. We thank Dr. Maritza G. J. Veprek-Heijman for valuable comments to the manuscript.

REFERENCES

[1] S. Veprek, A. Niederhofer, K. Moto et al. Surf. Coat. Technol., 2000, 133-134, P. 152-159. 2000.
[2] S. Veprek, M.G.J. Veprek-Heijman, P. Karvankova, J. Prochazka, Thin Solid Films, 2005, 476, P. 1-29.
[3] S. Veprek, R.F. Zhang, M.G.J. Veprek-Heijman et al. Surf. Coat. Technol., 2010, 204, P. 1898-1906.
[4] `S. Veprek, J. Nanosci. Nanotechnol. 2011, 11, P. 14-35.
[5] Y.-H.Chen, K.W.Lee, W.-A.Chiou et al. Surf.Coat.Tech., 2001, 146-147, P.209-214.
[6] S. Veprek, A.S. Argon, R.F. Zhang, Phil. Mag. Lett., 2007, 87, P. 955-966.
[7] R.F. Zhang, A.S. Argon, S. Veprek, Phys. Rev. B, 2010, 81, P. 245418-7.
[8] H. Söderberg, M. Odén, J.M. Molina-Aldareguia, L. Hultman, J. Appl. Phys., 2005, 97, P. 114327-8.
[9] L. Hultman, J. Barenõ, A. Flink et al. Phys. Rev. B, 2007, 75, P. 155437-6.
[10] H. Söderberg, M. Odén, T. Larsson et al. Appl. Phys. Lett., 2006, 88, P. 191902-3.
[11] H. Söderberg, M. Odén, A. Flink et al. J. Mater. Res., 2007, 22, P. 3255-3264.
[12] X. Hu, H. Zhang, J. Dai, G. Li, M. Gu, J. Vac.Sci. Techn. A, 2005, 23, P. 114-118.
[13] C. Iwamoto, S.-I. Tanaka, J. Am. Ceram. Soc., 1998, 81, P. 363-368.
[14] R.F. Zhang, A.S. Argon, S. Veprek, Phys. Rev. Lett., 2009, 102, P. 015503-4.
[15] R.F. Zhang, A.S. Argon, S. Veprek, Phys. Rev. B, 2009, 79, 245426-13.
[16] B. Alling, E.I. Isaev, A. Flink et al. Phys. Rev. B, 2008, 78, P. 132103-4.
[17] T. Marten, E.I. Isaev, B. Alling, L. Hultman, I.A. Abrikosov, Phys. Rev. B, 2010, 81, P. 212102-4.
[18] S. Hao, B. Delley, S. Veprek, C. Stampfl, Phys. Rev. Lett., 2006, 97, P. 086102-4.
[19] S. Hao, B. Delley, C. Stampfl, Phys. Rev. B, 2006, 74, P. 035402-12.
[20] S. Hao, B. Delley, C. Stampfl, Phys. Rev. B, 2006, 74, P. 035424-10.
[21] S. Baroni, A. Dal Corso, S. de Gironcoli et al. http://www.pwscf.org/.
[22] J.P. Perdew, K. Burke and M. Ernzerhof, Phys. Rev. Lett., 1996, 77, P. 3865- .
[23] D. Vanderbilt, Phys. Rev. B, 1990, 41, P. 7892- .
[24] S.R. Billeter, A. Curioni, W. Andreoni, Comput. Mater. Sci., 2003, 27, P. 437- .
[25] H.J. Monkhorst, and J.D. Pack, Phys. Rev. B, 1976, 13, P. 5188- .
[26] E.I. Isaev, S.I. Simak, I.A. Abrikosov et al. J. Appl. Phys., 2007, 101, P. 123519- .
[27] R.F. Zhang and S. Veprek, Phys. Rev. B, 2007, 76, P. 174105-6.